Table 2 Optimal nondimensional thickness distribution $u(x,y)$ for one quadrant of a simply supported square plate with fixed fundamental frequency of free vibration

x/y	0.0	0.167	0.333	0.5
		$u_{min}=0.6$		
0.0	1.593	1.161	0.6	0.6
0.167	1.161	1.253	0.6	0.6
0.333	0.6	0.6	0.6	0.888
0.5	0.6	0.6	0.888	1.017
		$u_{min}=0.8$		
0.0	1.425	1.196	0.8	0.8
0.167	1.196	0.8	0.8	0.8
0.333	0.8	0.8	0.995	0.984
0.5	0.8	0.8	0.984	1.118
		$u_{min}=0.9$		
0.0	1.263	1.103	0.9	0.9
0.167	1.103	0.9	0.9	0.9
0.333	0.9	0.9	1.005	0.982
0.5	0.9	0.9	0.982	1.054

Table 3 Effect of variation of the parameters ϵ_1 and ϵ_2 on the convergence of the method

ϵ_1	ϵ_2	Mass ratio	Objective function	Iterations
100.0	0.0001	0.91364	0.93501	111
10.0	0.0001	0.95315	0.95567	88
1.0	0.0001	0.95770	0.95796	100
0.1	0.0001	0.95816	0.95820	109
0.01	0.0001	0.95821	0.95822	137
0.001	0.0001	0.95821	0.95822	166
1.0	0.1	0.94029	0.94935	54
1.0	0.01	0.95602	0.95713	69
1.0	0.001	0.95754	0.95789	79
1.0	0.0001	0.95770	0.95796	100

square error in satisfying the partial differential equation of constraint is to be minimized (the partial differential equation is automatically satisfied at nodes (x_i,y_j) where $i=1$ or $j=1$).

The results of varying the minimum thickness constraint are presented in Table 1. The mass ratio provides a means of determining the weight savings for the optimal design. It is defined as the ratio of the mass of the optimal plate to that of the reference plate. Thus, weight savings of over 4%, 8%, and 19% were realized for the three respective minimum thickness constraints. In each case, the iterations required for convergence are tabulated for an initial guess corresponding to the reference plate. Convergence was assumed when the magnitude of the gradient of the objective function was less than 0.0001. The values of the optimal thickness distribution, $u(x,y)$, at the nodes of the grid for one quadrant of the plate are presented in Table 2 for each of the three minimum thickness constraints. The general tendency was for the mass to build up significantly at the corners of the plate and slightly at the center. Contour lines of the optimal thickness distributions for one quadrant of the plate are plotted in Fig. 1.

Table 3 illustrates the results of varying the magnitude of the parameters ϵ_1 and ϵ_2 for a minimum thickness constraint of $u_{min}=0.9$. A larger value of ϵ_1 implies a less severe penalty for violation of the differential equation of constraint, thus allowing a less accurate optimal thickness distribution and a smaller and less accurate value of the mass ratio. The value of the parameter ϵ_2 had to be kept relatively small in order to accurately satisfy the minimum thickness constraint. For practical purposes, a sufficiently accurate optimal solution can be obtained for $\epsilon_1=1.0$ and $\epsilon_2=0.001$.

Conclusions

The technique described herein has proven itself effective for the solution, via optimal control methodology, of an optimal structural design problem involving a two-dimensional structural member. The principle advantages are:

1) It avoids the direct solution of the partial differential equation of constraint.

2) The boundary conditions are automatically satisfied.

3) It is conceptually simple and easy to implement.

References

[1] Pierson, B. L., "A Survey of Optimal Structural Design Under Dynamic Constraints," *International Journal of Numerical Methods in Engineering*, Vol. 4, July-Aug. 1972, pp. 491-499.

[2] Olhoff, N., "Optimal Design of Vibrating Rectangular Plates," *International Journal of Solids and Structures*, Vol. 10, Jan. 1974, pp. 93-109.

[3] Armand, J.-L., "Applications of Optimal Control Theory to Structural Optimization: Analytical and Numerical Approach," paper presented at the IUTAM Symposium on Optimization in Structural Design, Polish Academy of Sciences, Warsaw, Poland, Aug. 1973.

[4] Haug, E. J., Pan, K. C., and Streeter, T. D., "A Computational Method for Optimal Structural Design II: Continuous Problems," *International Journal for Numerical Methods in Engineering*, Vol. 9, May-June 1975, pp. 649-667.

[5] Balakrishnan, A. V., "On a New Computing Technique in Optimal Control," *SIAM Journal on Control*, Vol. 6, May 1968, pp. 149-173.

[6] Foley, M. and Citron, S. J., "A Simple Technique for the Minimum Mass Design of Continuous Structural Members," *Journal of Applied Mechanics, Transactions of the ASME*, Vol. 44, June 1977, pp. 285-290.

[7] Timoshenko, S. and Woinowsky-Krieger, S., *Theory of Plates and Shells*, 2nd Ed., McGraw-Hill, New York, 1959, pp. 79-83.

[8] Lions, J. L., "Controle Optimal de Systemes Gouvernes par des Equations aux Derivees Partielles," Dunod, Paris, 1968, pp. 409-415.

[9] Balakrishnan, A. V., "A Computational Approach to the Maximum Principle," *Journal of Computer and System Sciences*, Vol. 5, April 1971, pp. 163-191.

Effect of Temperature-Dependent Heat Capacity on Aerodynamic Ablation of Melting Bodies

Anant Prasad*

Regional Institute of Technology, Jamshedpur, India

Nomenclature

c	= heat capacity per unit volume of the material
c_0	= heat capacity at melting temperature
h	= heat-transfer coefficient
H	= heat flow vector
k	= thermal conductivity of the material
L	= latent heat of the material
$q_1(t)$	= unknown surface temperature
$q_2(t)$	= unknown melting distance
t	= time
T_f	= temperature of the surroundings
α	= thermal diffusivity
β	= dimensionless temperature of the surroundings, c_0T_f/ρ_mL
γ	= dimensionless coefficient to give variation in heat capacity, λT_f
η	= dimensionless melting distance, hq_2/k

Received Jan. 31, 1978; revision received April 27, 1978.

Index categories: Heat Conduction; Ablation, Pyrolysis, Thermal Decomposition and Degradation.

*Assistant Professor, Department of Mechanical Engineering.

θ	= temperature distribution in the melt
λ	= coefficient to give variation in heat capacity
ρ_m	= density of the material at melting temperature
τ	= dimensionless time, $h^2 T_f t/\rho_m Lk$
ϕ	= dimensionless surface temperature, q_1/T_f

Introduction

MELTING of solid bodies due to aerodynamic heating is encountered as ablation of missiles and during spacecraft re-entry. The estimation of the rate of ablation of the solid protective layer, which is used to avoid the destruction of the principal parts in such situations, is essential in their design. An earlier investigation[4] suggests that it depends upon heat capacity of the melting solids occurring in the single independent parameter β that controls the melting, and on the rate of heat transfer which is determined by the solids' conductivity. During ablation change in heat capacity due to rise in temperature, therefore, bears a significant effect on melting in comparison with temperature-dependent conductivity. The mathematical model of this problem gives governing differential equation and nonlinear boundary condition. In the literature, its closed-form solution is not reported, although a number of approximate methods are available to analyze such a problem. Several workers[1-7] in the past employed one of these methods, called Biot's variational method, to solve melting problems with the thermophysical properties of the melting solids uniform and the melt not removed. These problems were also investigated using a heat balance integral method.[8] Variation in thermophysical properties of melting solids was taken by Biot and Agrawal[9] to find the rate of melting and associated parameters for sudden removal of melt. The metling occurred by uniform heat flux heating.

This Note describes the effect of temperature-dependent heat capacity on the behavior of ablation and temperature buildup at the surface when ablation in a melting solid occurs due to aerodynamic heating. Using a variational principle,[10] its results are obtained in closed form. Numerical solutions are also presented.

Formulation of the Problem

The melting body is taken to be a semi-infinite solid of constant cross-sectional area. Its thermophysical properties are temperature-dependent above melting temperature except the thermal conductivity which is assumed to be constant. As a result, the heat capacity has different values in the solid and molten regions, whereas the value of thermal conductivity remains the same in both regions. This is true in view of the discussion just mentioned. After initiation of melting, T_f and $q_1(o,t)$ are the temperature of surroundings and the surface of the melt, respectively, and $q_2(t)$ is taken as the distance of the melt line from the surface after time t which is measured from the initiation of melting. Although there exists a temperature distribution in the solid, this problem is simplified by assuming the entire solid at melting temperature. The validity of this assumption was shown earlier.[8] It is, therefore, governed by the equation

$$c(\theta)\partial^2\theta/\partial x^2 = k\partial\theta/\partial t \quad x>0,\ t>0 \tag{1}$$

and the related initial and boundary conditions are

$$\theta=0,\ q_2(t)=0 \qquad t=0 \tag{2}$$

$$-k\partial\theta/\partial x = h(T_f-q_1) \qquad x=0,\ t>0,\ T_f>q_1 \tag{3}$$

$$\dot{H}=\rho_m L\dot{q}_2 \qquad x=q_2,\ t>0 \tag{4}$$

$\dot{H}$ in Eq. (4) denotes the rate of heat flow with $H=\rho_m Lq_2$. This equation is also obtained by applying the principles of conservation of energy at the interface of the melt line with the melting temperature taken to be zero and the solid assumed to be at uniform temperature.

Solution

A linear temperature distribution is considered in the melt as

$$\theta = q_1(1-x/q_2) \tag{5}$$

where the instant surface temperature q_1 and the instant melting distance q_2 are unknown generalized coordinates to be determined as the function of time. The conservation of energy for temperature-dependent heat capacity is

$$\mathrm{Div}H = -\int_0^\theta c\,\mathrm{d}\theta \tag{6}$$

In the present problem, the heat capacity c is assumed to be a linear function of temperature

$$c = c_0(1+\lambda\theta) \tag{7}$$

with the value of c_0 at melting temperature.

Equation (5) together with Eqs. (6) and (7) yields the heat flowfield

$$H = \tfrac{1}{2}c_0q_1q_2(1-x/q_2)^2 + (1/6)c_0\lambda q_1^2 q_2(1-x/q_2)^3 + \rho_m Lq_2 \tag{8}$$

This satisfies the boundary condition [Eq. (4)].

As the temperature distribution [Eq. (5)], and heat flowfield [Eq. (8)] are known, the Lagrangian equation based on Biot's variational principle is employed

$$\partial V/\partial q_2 + \partial D/\partial \dot{q}_2 = Q_2 \tag{9}$$

where the function V represents the thermal potential

$$V = \int_0^{q_2}\left(\int_0^\theta c\theta\,\mathrm{d}\theta\right)\mathrm{d}x \tag{10}$$

D, the thermal dissipation

$$D = (1/2k)\int_0^{q_2}\dot{H}^2\,\mathrm{d}x \tag{11}$$

and Q_2, the thermal force

$$Q_2 = (\theta)_{x=0}(\partial H/\partial q_2)_{x=0} \tag{12}$$

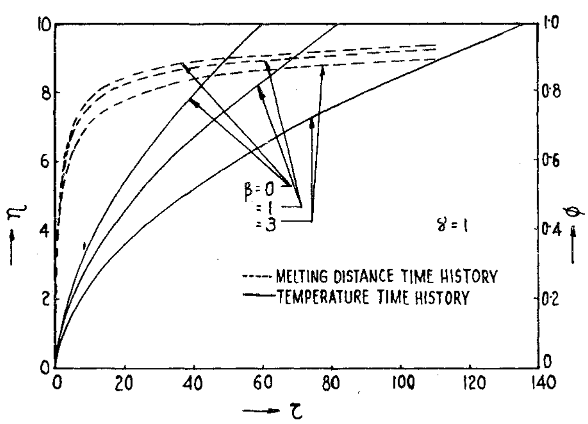

Fig. 1 Behavior of surface temperature and melting distance with time for different values of β and γ taken as a parameter.

Substituting Eqs. (5) and (8) into Eq. (9) gives

$$(q_2\dot{q}_2/2k)[2\rho_m^2L^2+4c_0\rho_mLq_1/3+q_1^2(4c_0^2/15+c_0\lambda\rho_mL/3)+3c_0^2\lambda q_1^3/20+13c_0^2\lambda^2q_1^4/630]+(\dot{q}_1q_2^2/2k)$$
$$\times[c_0\rho_mL/3+q_1(3c_0^2/20+c_0\lambda\rho_mL/6)+11c_0^2\lambda q_1^2/90+c_0^2\lambda^2q_1^3/42]=\rho_mLq_1+c_0q_1^2/3+c_0\lambda q_1^3/12 \quad (13)$$

Eqs. (5) and (3) yield a relationship between the surface temperature q_1 and the melting distance q_2

$$q_2=kq_1/h(T_f-q_1) \quad (14)$$

This equation introduces an additional relation between the generalized coordinates and reduces the number of differential equations of Lagrangian type by one.

Using the nondimensional quantities from the nomenclature, the combination of Eqs. (13) and (14) yields

$$\dot{\phi}(A_0+A_1\phi+A_2\phi^2+A_3\phi^3+A_4\phi^4+A_5\phi^5)=210(1-\phi)^3(B_0+B_1\phi+B_2\phi^2) \quad (15)$$

where

$$A_0=2520,\quad A_1=2100\beta,\quad A_2=105(5\beta^2-4\beta-6\beta\gamma),\quad A_3=7(49\beta^2\gamma-30\beta\gamma-27\beta^2),$$
$$A_4=2(28\beta^2\gamma^2-77\beta^2\gamma),\quad A_5=-30\beta^2\gamma^2,\quad B_0=12,\quad B_1=4\beta,\quad B_2=\beta\gamma$$

By solving Eq. (15), the behavior of surface temperature with time is obtained in closed form.

$$\tau=(1/210)[L_1\ln(1-\Phi)+(L_2-L_3)\Phi+L_4(\Phi/(1-\Phi))+L_5\Phi(2-\Phi)/(1-\Phi)^2+L_6\ln\{B_1+(B_1^2-4B_0B_2)^{1/2}\}$$
$$\times\{2B_2\Phi+B_1-(B_1^2-4B_0B_2)^{1/2}\}/\{B_1-(B_1^2-4B_0B_2)^{1/2}\}\{2B_2\Phi+B_1+(B_1-4B_0B_2)^{1/2}\}+L_7\ln(B_0+B_1\Phi+B_2\Phi^2)/B_0] \quad (16)$$

where

$$L_1=2c_2+3c_3-c_1-d_1+d_2-d_3,\quad L_2=c_5/B_2-c_1,\quad L_3=-(c_2+c_3),\quad L_4=(c_2+3c_3+d_2-2d_3),\quad L_5=\tfrac{1}{2}(d_3-c_3),$$
$$L_6=d_4-(B_1/2B_2)\{c_4+d_5-(c_5/B_2)(B_1^2-2B_0B_2)\}]/(B_1^2-4B_0B_2)^{1/2},\quad L_7=(1/2B_2)(c_4-c_5B_1/B_2+d_5)$$

and

$$c_1=[(3A_1+A_2-A_5)(B_2-B_0)(\Sigma B_i)+(\Sigma A_i)\{B_0(B_0+B_1)+B_2(B_1+B_2)\}-(A_3+A_4-2A_1)(B_0+B_2)(\Sigma B_i)]/L$$
$$c_2=[(A_3+A_4-2A_1)/(B_2-B_0)][1-(B_0+B_2)\{(B_2-B_0)+(\Sigma B_i)^2\}/L]+(\Sigma A_i)/(\Sigma B_i)(B_2-B_0)$$
$$\times[\{B_0(B_0+B_1)+B_2(B_1+B_2)\}\{(B_2-B_0)+(\Sigma B_i)^2\}/L-(B_0+B_2)]+(3A_1+A_2-A_5)\{(B_2-B_0)+(\Sigma B_i)^2\}/L$$
$$c_3=(A_3+A_4-2A_1)(B_2^2-B_0^2)/L-(3A_1+A_2-A_5)(B_2-B_0)^2/L+(\Sigma A_i)/(\Sigma B_i)$$
$$\times[1-(B_2-B_0)\{B_0(B_0+B_1)+B_2(B_1+B_2)\}/L]$$
$$c_4=A_1-B_0[(3A_1+A_2-A_5)(B_2-B_0)(\Sigma B_i)/L+(\Sigma A_i)\{B_0(B_0+B_1)+B_2(B_1+B_2)\}/L$$
$$-(A_3+A_4-2A_1)(B_0+B_2)/(\Sigma B_i)/L]$$
$$c_5=A_5+(A_3+A_4-2A_1)[B_2/(B_2-B_0)-B_2(B_2+B_0)(1+B_2-B_0)/L-B_2(B_2+B_0)(B_1+2B_0)$$
$$\times(\Sigma B_i)/(B_2-B_0)L+(\Sigma A_i)/(\Sigma B_i)[B_2(1+B_2-B_0)\{B_0(B_0+B_1)+B_2(B_1+B_2)\}/L$$
$$+B_2\{B_0(B_0+B_1)+B_2(B_1+B_2)\}(B_1+2B_0)(\Sigma B_i)/(B_2-B_0)L-B_2(B_1+B_2)/(B_2-B_0)]$$
$$+(3A_1+A_2-A_5)[B_2(B_2-B_0)(1+B_2-B_0)/L-B_2(B_1+2B_0)(\Sigma B_i)/L]$$
$$d_1=2A_0B_2(\Sigma 3B_i-B_0)/L,\quad d_2=\{A_0/(B_2-B_0)\}\{1+B_2/(\Sigma B_i)\}+\{2A_0(B_1+B_2)(B_2+\Sigma B_i)/L\}\{1/\Sigma B_i+\Sigma B_i/(B_2-B_0)\}$$
$$d_3=A_0/\Sigma B_i-A_0B_2(B_2-B_0)(6-2B_0/\Sigma B_i)/L,\quad d_4=A_0-2B_0A_0\{(\Sigma B_i)(B_0+3B_2)-B_0B_2\}/L$$
$$d_5=2A_0B_2(B_0/\Sigma B_i-3)/(B_2-B_0)+A_0B_2/L\{(1+B_2-B_0)\}\{B_0(\Sigma B_i-B_2-1)+B_2(\Sigma B_i+5-B_0)\}$$
$$+(B_1+2B_0)(\Sigma B_i)+\{3A_0B_2(B_2+2B_0)/(B_2-B_0)L\}\{\Sigma B_i(B_0+B_2)-B_0B_2\}$$
$$\Sigma A_i=A_0+A_1+A_2+A_3+A_4+A_5,\quad \Sigma B_i=B_0+B_1+B_2,\quad L=(B_2-B_0)\{B_0(1-B_2)+B_2(1+B_2)\}+\Sigma B_i\{2B_1B_2+(B_0+B_2)^2\}$$

If the heat capacity does not vary with temperature, λ becomes zero and Eq. (16) reduces to the same simple solution obtained earlier.[4] Also, for very high latent heat ($L\to\infty$, $\beta\to 0$), Eq. (16) yields

$$\tau=\tfrac{1}{2}[1/(1-\phi)^2-1] \quad (17)$$

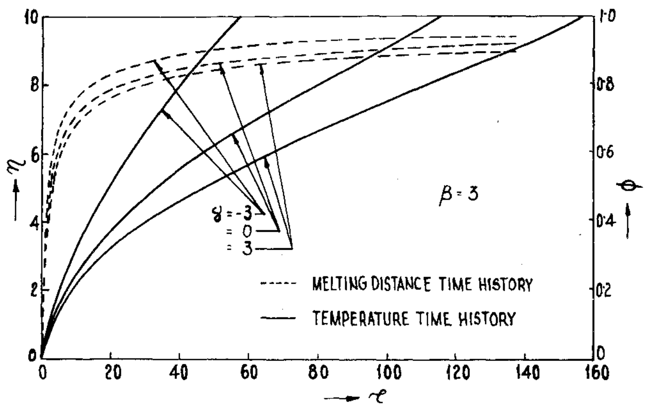

Fig. 2 Effect of variation in γ on melting distance time history and surface temperature time history for a particular value of β.

Using the nondimensional form of Eq. (14), Eq. (17) in terms of melting distance is:

$$\tau = \eta^2/2 + \eta \tag{18}$$

This is the same expression obtained by the heat balance integral method[8] using parabolic temperature profile in the melt and Biot's variational method[4] using linear temperature profile [Eq. (5)].

To find the numerical solution, Eq. (15) is numerically integrated between the limit of Φ varying from 0 to 1 using Simpson's formula and the limit is divided into 100 parts with the value of each part being equal to 0.01. This yielded reliable results.

Figure 1 presents surface temperature $\phi(\tau)$ and melting distance $\eta(\tau)$ as a function of time with γ as a parameter for different values of β which, for quartz and graphite used as ablating materials,[11] become, respectively, 6.05×10^{-4} and 1.244×10^{-4} per degree Kelvin rise in temperature above their respective melting temperature. It shows that both of them increase with an increase in time for any β, whereas they decrease with increase in β at any time. Similar behavior was also observed for other values of γ. Figure 2 illustrates the time-variant surface temperature $\phi(\tau)$ and melting distance $\eta(\tau)$ for variable heat capacity for a particular value of β. Negative and positive γ correspond, respectively, to decrease and increase in heat capacity with rise in temperature, whereas $\gamma = 0$ represents the heat capacity invariant with change in temperature. It is seen that as γ changes from -3 to $+3$ more time is required to obtain the same $\eta(\tau)$ and $\phi(\tau)$ at a higher value of γ. This is true for all values of β except $\beta = 0$ for which these predictions do not depend on γ, as is evident from Eqs. (17) and (18).

Conclusion

A variational method of solution has been employed to predict the surface temperature time history and melting distance time history during ablation of melting solids due to aerodynamic heating. It takes into account the effect of temperature-dependent heat capacity of solids on ablation.

References

[1] Biot, M. A. and Daughaday, H., "Variational Analysis of Ablation," *Journal of Aerospace Sciences*, Vol. 29, Feb. 1962, pp. 227-229.

[2] Lardner, T. J., "Approximate Solution to Phase-Change Problems," *AIAA Journal*, Vol. 5, Nov. 1967, pp. 2079-2080.

[3] Prasad, A. and Agrawal, H. C., "Biot's Variational Principle for a Stefan Problem," *AIAA Journal*, Vol. 10, March 1972, pp. 325-327.

[4] Prasad, A. and Agrawal, H. C., "Biot's Variational Principle for Aerodynamic Ablation of Melting Solids," *AIAA Journal*, Vol. 12, Feb. 1974, pp. 250-252.

[5] Prasad, A. and Sinha, S. N., "Radiative Ablation of Melting Solids," *AIAA Journal*, Vol. 14, Oct. 1976, pp. 1494-1497.

[6] Prasad, A. and Ajit, S. J., "A Variational Analysis of Solidification in Continuous Casting," *Transactions of IIM*, Vol. 29, No. 6, Dec. 1976, pp. 438-441.

[7] Prasad, A., Pathak, B. P. and Ajit, S. J., "Solidification in an Axisymmetric Mold of a Continuous Casting Machine," *Fourth National Heat Mass Transfer Conference Proceeding of India*, Nov. 1977, 4HMT 51, pp. 469-475.

[8] Goodman, T. R., "The Heat Balance Integral and Its Application to Problems Involving a Change of Phase," *Transactions of the ASME*, Vol. 80, Feb. 1958, pp. 335-342.

[9] Biot, M. A. and Agrawal, H. C., "Variational Analysis of Ablation for Variable Properties," *Transactions of the ASME, Journal of Heat Transfer*, Series C, Vol. 86, 1964, pp. 437-442.

[10] Biot, M. A., "Variational Principle in Heat Transfer, "Oxford University Press, London, 1970, pp. 85-92.

[11] Rohsenow, W. M. and Hartnett, J. P., "*Hand Book of Heat Transfer,* McGraw Hill, N.Y., 1973, pp. 16-49.

Unsteady Three-Dimensional Compressible Stagnation-Point Boundary Layers

G. Nath* and M. Kumari†
Indian Institute of Science, Bangalore, India

Introduction

THE solution of many practical problems in fluid dynamics requires the understanding of unsteady three-dimensional compressible boundary layers. The unsteady laminar two-dimensional and axisymmetric compressible boundary layers for constant $\rho\mu$ flows ($\rho \alpha T^{-1}$, $\mu \alpha T$, σ=constant where ρ, σ, μ, and T are the density, Prandtl number, viscosity, and temperature, respectively), when the incident freestream varies arbitrarily with time, have been studied by several authors[1-5] using momentum-integral or series-expansion methods. Recently, Vimala and Nath[6] restudied the two-dimensional stagnation-point flow problem for constant $\rho\mu$ flows using an implicit finite-difference scheme.

In the present Note, the unsteady three-dimensional laminar compressible stagnation-point boundary layers for variable $\rho\mu$ flows ($\rho \alpha T^{-1}$, $\mu \alpha T^{\omega}$, σ=constant where ω is the index of the power-law variation of viscosity) have been studied when the wall temperature and the incident stream vary arbitrarily with time. The equations governing the flow have been solved numerically using an implicit finite-difference scheme.[6,7] Computations have been carried out for the incident stream which moves with constant acceleration and fluctuates about a steady mean, and for the wall temperature decreasing with time.

Governing Equations

The governing equations in dimensionless form for the unsteady laminar compressible boundary-layer at a three-dimensional stagnation point for variable $\rho\mu$ flows, under the assumptions that 1) the incident stream and wall temperature vary arbitrarily with time, 2) the dissipation terms are negligible at the stagnation point, and 3) the external flow is

Received March 6, 1978.

Index categories: Boundary Layers and Convective Heat Transfer—Laminar; Nonsteady Aerodynamics.

*Associate Professor, Dept. of Applied Mathematics.
†Research Student, Dept. of Applied Mathematics.